

---

This is an electronic reprint of the original article.  
This reprint may differ from the original in pagination and typographic detail.

Murashko, Kirill; Kortelainen, Miika; Hu, Tao; Kobets, Anna; Kallio, Tanja; Lassi, Ulla; Lähde, Anna

## Tuning of the Single Crystal NMC811 Properties Synthesized from Metal Sulfate Precursors by Spray Drying and Thermal Treatment Methods

*Published in:*  
Journal of the Electrochemical Society

*DOI:*  
[10.1149/1945-7111/ae0072](https://doi.org/10.1149/1945-7111/ae0072)

Published: 08/09/2025

*Document Version*  
Publisher's PDF, also known as Version of record

*Published under the following license:*  
CC BY

*Please cite the original version:*  
Murashko, K., Kortelainen, M., Hu, T., Kobets, A., Kallio, T., Lassi, U., & Lähde, A. (2025). Tuning of the Single Crystal NMC811 Properties Synthesized from Metal Sulfate Precursors by Spray Drying and Thermal Treatment Methods. *Journal of the Electrochemical Society*, 172(9), Article 090512. <https://doi.org/10.1149/1945-7111/ae0072>

---

This material is protected by copyright and other intellectual property rights, and duplication or sale of all or part of any of the repository collections is not permitted, except that material may be duplicated by you for your research use or educational purposes in electronic or print form. You must obtain permission for any other use. Electronic or print copies may not be offered, whether for sale or otherwise to anyone who is not an authorised user.

**OPEN ACCESS**

## Tuning of the Single Crystal NMC811 Properties Synthesized from Metal Sulfate Precursors by Spray Drying and Thermal Treatment Methods

To cite this article: Kirill Murashko *et al* 2025 *J. Electrochem. Soc.* **172** 090512

View the [article online](#) for updates and enhancements.

### You may also like

- [Understanding the Cathodic Overpotential in  \$\text{LiMn}\_2\text{O}\_4\$  Electrodes for Lithium Recovery from Brines in a Continuous Flow-by Electrochemical Reactor](#)  
Clara Roggerone, Fabio La Mantia, Julia Kowal *et al.*
- [Understanding Lithium Deposition in Lithium-Ion Batteries: The Link between Impedance Results and Electrochemical Behavior](#)  
Andrea Kinberger, Tom R  ther, Leonard Jahn *et al.*
- [Microstructure-Tuned Hydrogen Embrittlement in 7050 Aluminum Alloy: Combined Impedance Analysis and Advanced Characterization](#)  
Mingyang Wang, Yuanyuan Ji, Digby D. Macdonald *et al.*

## ECC-Opto-10 Optical Battery Test Cell: Visualize the Processes Inside Your Battery!

**EL-CELL**<sup>®</sup>  
electrochemical test equipment

- ✓ **Battery Test Cell for Optical Characterization**  
Designed for light microscopy, Raman spectroscopy and XRD.
- ✓ **Optimized, Low Profile Cell Design (Device Height 21.5 mm)**  
Low cell height for high compatibility, fits on standard samples stages.
- ✓ **High Cycling Stability and Easy Handling**  
Dedicated sample holders for different electrode arrangements included!
- ✓ **Cell Lids with Different Openings and Window Materials Available**

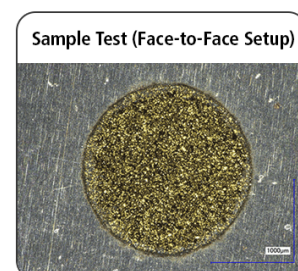
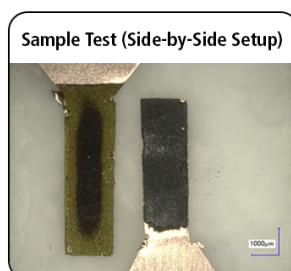


**Contact us:**

☎ +49 40 79012-734

✉ [sales@el-cell.com](mailto:sales@el-cell.com)

🌐 [www.el-cell.com](http://www.el-cell.com)





# Tuning of the Single Crystal NMC811 Properties Synthesized from Metal Sulfate Precursors by Spray Drying and Thermal Treatment Methods

Kirill Murashko,<sup>1,z</sup>  Miika Kortelainen,<sup>1</sup> Tao Hu,<sup>2</sup> Anna Kobets,<sup>3</sup> Tanja Kallio,<sup>3</sup> Ulla Lassi,<sup>2</sup> and Anna Lähde<sup>1</sup>

<sup>1</sup>Fine Particle and Aerosol Technology Laboratory, Department of Environmental and Biological Sciences, University of Eastern Finland, 70210 Kuopio, Finland

<sup>2</sup>Research Unit of Sustainable Chemistry, University of Oulu, PO Box 3000, FI-90014 University of Oulu, Finland

<sup>3</sup>Department of Chemistry and Materials Science, School of Chemical Engineering, Aalto University, Espoo, 02150, Finland

Diversification of the lithium-ion battery material production is one of the important challenges for the modern world to improve the sustainability of the lithium-ion battery technology. The introduction of novel methods for the materials' production can help to find a solution to this challenge. In the presented work, we investigated the preparation of single-crystal Ni-rich  $\text{LiNi}_{0.8}\text{Co}_{0.1}\text{Mn}_{0.1}\text{O}_2$  (SC-NMC) cathode material from a metal sulphates water solution by a facile and robust three-step method, which includes a spray drying technique followed by solid-state calcination and lithiation steps. The calcination process was analyzed with and without the presence of a lithium salt, and the effect of the salt amount on the parameters of the synthesized material is described. In addition, the optimization of the lithiation processes is presented, which allows the preparation of the SC-NMC cathode material with highly dispersed single-crystal morphology, relatively small grain size and good electrochemical properties, which are similar to properties of the polycrystalline NCM811 produced by the conventional co-precipitation method. The results presented emphasize the importance of cathode material synthesis with preferred particle size and orientation to enhance the Li-ion diffusion pathway, specific capacity and cycling stability of the produced cathode material.

© 2025 The Author(s). Published on behalf of The Electrochemical Society by IOP Publishing Limited. This is an open access article distributed under the terms of the Creative Commons Attribution 4.0 License (CC BY, <https://creativecommons.org/licenses/by/4.0/>), which permits unrestricted reuse of the work in any medium, provided the original work is properly cited. [DOI: 10.1149/1945-7111/ae0072]



Manuscript submitted May 20, 2025; revised manuscript received July 23, 2025. Published September 8, 2025.

Supplementary material for this article is available [online](#)

Currently, the layered  $\text{LiNi}_x\text{Mn}_y\text{Co}_z\text{O}_2$  (NMC) cathode materials are the most widely used for the creation of cathodes for high-energy-density Li-ion batteries.<sup>1</sup> Co-precipitation technology is a most popular large-scale technology for NMC precursor (NMC hydroxide (NMC-OH)) synthesis because this method allows the production of NMC-OH with uniform particle size from metal sulfates. The selection of the metal sulfates for the NMC precursor synthesis is conditioned by the mining process of the nickel, which right now is dominantly obtained from sulfide ore in the form of nickel sulfate. Although metal sulfates are currently the cheapest option for NMC precursor production, the co-precipitation technology is a complex technology, which includes many process steps, high water consumption and a significant amount of hard-to-process side product that leads to the ultimately high production cost. Especially in countries with strict environmental regulations, the treatment of the residual water obtained after NMC precursor co-precipitation and contaminated with sodium sulfate with a concentration of  $1\text{--}2\text{ mol}\cdot\text{l}^{-1}$ , may significantly affect the overall cost of the synthesis process. In general, about 1.3 kg of sodium sulfate is produced per 1 kg of NMC-OH during the co-precipitation process, which cannot be dumped with the wastewater because of the legal limits on the discharge of sodium sulfate solution in many countries.<sup>2</sup> The lime precipitation process, where the addition of hydrated lime precipitates most of the sulfate as gypsum, can be used to decrease the sulfate concentration but even in this case the additional costs still will be added to the overall process. Also, the received calcium sulfate should be additionally treated or recycled as it cannot be reused in the manufacture of NMC precursor.<sup>2</sup> Because of this, the interest in other technologies for NMC production such as solid-gel, solid-state, hydrothermal, spray-based methods, and combustion methods is increasing.

Among all alternative technologies for NMC precursor production, spray-based methods are attractive for the large-scale continuous production of rounded particles with a narrow size distribution due to their good metal mixing ability, good scalability, affordability, performance, and cost-effectiveness.<sup>3,4</sup> The synthesis of the NMC precursor

by using spray-based methods (e.g. spray drying and pyrolysis, flame spray pyrolysis, etc) was previously intensively considered by many researchers. The spray drying technologies with followed calcination and lithiation were presented for the NMC synthesis in Refs. 5–7. The spray pyrolysis and flame-assisted spray pyrolysis methods were considered for the nickel-rich NMC production in Refs. 8–12. However, all presented spray-based methods are based on the use of relatively expensive metal salts, for example, metal nitrates, metal chloride or metal acetates. The use of metal sulfates for the synthesis of the NMC during the one-step spray pyrolysis process is rarely considered as lithium oxide reacts with sulphur to produce  $\text{Li}_2\text{SO}_4$  and a high temperature should be applied to decompose the  $\text{Li}_2\text{SO}_4$ . Especially in the case of the Ni-rich cathode materials the high temperature will aggravate cations disordering and deteriorate their electrochemical properties.<sup>13</sup> Moreover, the high temperature leads to the significant sintering and formation of the single-crystal (SC) cathode materials with overlarge grain size (3–10  $\mu\text{m}$ ) and rarely exposed  $\text{Li}^+$  diffusion planes (i.e., {010} planes) which significantly restricts the rate capability of the produced materials.<sup>14</sup> Therefore, to be able to use metal sulfates for the preparation of the NMC, the multiple-step method is usually necessary.

In this work, we investigated the preparation of single-crystal Ni-rich  $\text{LiNi}_{0.8}\text{Co}_{0.1}\text{Mn}_{0.1}\text{O}_2$  (SC-NMC) cathode material from a metal sulphates water solution by a facile and robust three-step method, which includes a spray drying technique followed by solid-state calcination and lithiation steps. In general, the calcination process can be combined with the spray drying technique but, in this work, it was considered as the separate step to understand its effect on synthesized material properties. The calcination process was precisely analyzed, with and without the presence of a lithium salt, and the effect of the salt amount on the parameters of the synthesized material is described. In addition, the optimization of the lithiation processes was done, which allows the preparation of the SC-NMC cathode material with highly dispersed single-crystal morphology, relatively small grain size and good electrochemical properties, which are similar to properties of the polycrystalline NCM811 produced by the conventional co-precipitation method.

<sup>z</sup>E-mail: kirill.murashko@uef.fi

## Materials and Methods

**Materials synthesis.**—The metal sulphates water solution (1.5 M  $\text{MeSO}_4$ ) was prepared from industrial-grade raw materials in deionized water. The precursor solution was aerosolised using an ultrasonic nebuliser (Pyrosol 7901, RBI instrumentation). Air was employed to carry the droplet stream in a tube furnace consisting of five tubes. The flow rate of the air in each tube was  $1.5 \text{ l min}^{-1}$ . liquid droplets were then dried in the heated zone of the reactor at a temperature of  $160^\circ\text{C}$  with a residence time of 10 s. The spray-dried NMC-sulphate particles were collected on a bag filter. The calcination process was used to convert the NMC-sulphate to NMC-oxide structures. For the calcination process, the obtained NMC-sulfate was mixed with LiOH at different lithium to transition metals (Li/TM (TM=Ni, Co, Mn)) molar ratios (0, 0.1, 0.2, 0.3, 0.5 and 0.9), placed in the alumina boat and calcined in an air atmosphere. The addition of the LiOH was done to investigate the reactions that occurred during the heating of NMC-sulfate with a lithium source. The calcination of the powder was done in three steps by using  $450^\circ\text{C}$  for 2 h,  $670^\circ\text{C}$  for 3 h and  $830^\circ\text{C}$  for 12 h. The powder was ground manually between each step. The three heating and hand-mixing steps were applied during calcination to ensure the good mixing efficiency of the spray-dried NMC-sulphate particles with lithium salt. After calcination, the powder was washed with water and dried to remove the lithium salt from the powder, and it was lithiated by a similar approach presented by Lui et al.<sup>15</sup> During lithiation two-steps were used to produce layered single crystal  $\text{LiNi}_x\text{Mn}_y\text{Co}_z\text{O}_2$  cathode material further denoted as SC-NMC. In the first step, the precursor was mixed with LiOH (LiOH anhydrous, 98% purity, Alfa Aesar) in the 0.975 li/TM molar ratio. The mixtures were ground together by mortar and pestle until homogenous (about 10 min). The sample was first preheated in a furnace for 3 h at  $450^\circ\text{C}$  before a second round of grinding. Further, the sample was heated in the furnace for 10 h at  $860^\circ\text{C}$  in oxygen flow. In the second step, LiOH was added to the sample to reach 1.05 overall Li/TM ratio and ground together until homogenous. The sample was heated in the furnace at  $750^\circ\text{C}$  for 12 h in oxygen flow. The temperature during the lithiation process was measured by a thermocouple inserted into the oven close to the treated sample.

The polycrystalline NCM811 was produced by using the coprecipitation method and lithiated by using similar procedures as it was done in Ref. 16. The produced material was denoted as PC-NMC and used only as a reference sample.

**Materials characterization.**—Thermogravimetric analysis (TGA) (Q50, TA instruments, USA) of the initial spray-dried NMC-sulphate powder was performed in air to obtain the weight percentage of the different components in the sample. The microstructure and morphology of samples were determined using a field emission scanning electron microscope (Zeiss Sigma HD/VP FE-SEM) equipped with energy-dispersive X-ray spectroscopy (EDS, Thermo Scientific Noran System 7). The average particle size estimation was done based on the SEM images using the ImageJ program. The probability density function was calculated after measuring at least 150 particles. The surface morphology was measured with an SE2 detector at an accelerating voltage of 2 kV for the spray-dried NMC sulfate powder and 10 kV for the rest considered samples. The elemental composition was examined at 15 kV.

The isopropanol absorption bottle method was used in this study to determine the  $\text{SO}_2$  and  $\text{SO}_3$  concentrations in the outlet gases during the calcination process. This method is based on the EPA Method 8,<sup>17</sup> but with some modifications. The flue gas obtained during the calcination of 2 grams of spray-dried NMC-sulphate powder was directed to the gas absorption system with the 3 lpm flow rate and was first bubbled through one impinger filled with 100 ml of 80 vol% isopropanol solution (diluted in water) to absorb  $\text{SO}_3/\text{H}_2\text{SO}_4$ , then through three impingers filled with 100 ml of 3 vol%  $\text{H}_2\text{O}_2$  solution to absorb  $\text{SO}_2$ . The third bottle with 3 vol.%  $\text{H}_2\text{O}_2$  solution was used to confirm the complete absorption of the

$\text{SO}_2$  in previous bottles. The pH level in the last bottle was checked by a pH indicator strip. The amount of sulphate in the solutions was determined immediately after the collection to minimize the oxidation of  $\text{SO}_2$  in the isopropanol solution. The determination of sulphate ions was done by titration with barium chloride and using thorin as an indicator.

The phases and structure were analyzed with Rigaku SmartLab 9 kW X-ray diffractometer (XRD) using  $\text{CuK}\alpha$  1.54059 as source at 45 kV and 200 mA. Diffractograms were collected in the  $2\theta$  range of  $5\text{--}130^\circ$  at  $0.02^\circ$  intervals and scan speed of  $4.06 \text{ deg min}^{-1}$ . The composition of the material was identified using the PDXL2 software (Rigaku), employing the Whole Powder Pattern Fitting (WPPF) method. Rietveld refinement was carried out using the FullProf program package. Pseudo-Voigt function was employed as a peak shape function.

The in situ HT-XRD phase analysis was performed with an X'Pert Pro MPD Powder XRD (Malvern Panalytical, Cu-K 1) combined with a high-temperature oven HTK 1200 N (Anton Paar GmbH). The LiOH (5% excess) was grounded in the mortar and then mixed with NMC precursor. The obtained mixture was placed in the sample holder for in situ HT-XRD measurement. The XRD data was collected in a temperature range between  $100^\circ\text{C}$  and  $900^\circ\text{C}$ , in increments of  $50^\circ\text{C}$ . Each step involves a 1 h dwell period, followed by a 1 h measurement from  $2\theta = 10^\circ$  to  $70^\circ$ . The measurements were conducted in an oxygen atmosphere.

Concentrations of trace elements were measured by inductively coupled plasma optical emission spectrometry (ICP-OES) using an Agilent 5110 SVDV (Agilent Technologies Inc., Santa Clara, California, USA). The samples were digested using MARSX Microwave oven (CEM Corporation, USA). The samples (30 mg) and 9 ml 69%  $\text{HNO}_3$  + 3 ml 37%  $\text{HCl}$  were added into the microwave vessels and heated at  $180^\circ\text{C}/10 \text{ min}$  according to EPA3051A method. The resulting solutions were filtered and diluted to 50 ml with ultrapure water in a volumetric flask. The samples were then analyzed with ICP-OES. Axial measuring mode was used for the analysis. Four replicate measurements were carried out for each sample, and 2% nitric acid was used for rinsing 30 s between samples. Preceding the measurement of each sample was a 25 s flush time (during which the sample was pumped to the plasma at a faster flow rate) and a 10 s delay time. A correlation coefficient of  $>0.9995$  was required for the calibration. Standard and blank samples were measured at the beginning and at the end of the measurements for quality control purposes.

Specific surface area and pore distributions were determined from the adsorption-desorption isotherms using nitrogen as adsorbate. Determinations were performed by the Micromeritics ASAP 2020 instrument (Norcross, USA). Portions of each sample (100–200 mg) were degassed at low pressure ( $2 \mu\text{m Hg}$ ) and at the temperature of  $140^\circ\text{C}$  for two hours to clean the surfaces and remove any adsorbed gases. Adsorption isotherms were obtained by immersing sample tubes in liquid nitrogen ( $-196^\circ\text{C}$ ) to achieve constant temperature conditions. Gaseous nitrogen was then added to the samples in small doses, and the resulting isotherms were obtained. Specific surface areas were calculated from adsorption isotherms according to the BET method, while nitrogen adsorption and desorption isotherms were used to calculate the pore size distribution using the DFT (Density Functional Theory) algorithm.

**Electrochemical measurements/characterization.**—The created SC-NMC cathode material was first sieved by  $45 \mu\text{m}$  sieve. The composition of the slurry was 4 wt% PVDF binder (KYNAR HSV 1810), 4 wt% conductive carbon (TIMCAL C65) and 92 wt% SC-NMC. The slurry was coated on the aluminium foil with  $160 \mu\text{m}$  and then dried in the vacuum oven at  $120^\circ\text{C}$  for 12 h. The dried electrodes were calendared by MSK-2150 (MTI KJ group, China). The average active material mass loading on the foil was about  $9 \text{ mg/cm}^2$ . The electrochemical performance of the produced electrodes was measured by using coin cells. The coin cells were

subsequently assembled in an Ar-filled glove box. The metallic lithium was used as the counter electrode. 1 M LiPF<sub>6</sub> in 1:1 ethylene carbonate (EC)/dimethyl carbonate (Sigma-Aldrich, battery grade) and glass microfiber filters (Whatman GF/A) were used as the electrolyte and separator, respectively. The galvanostatic charge-discharge performances of all assembled cells were measured between 2.8 and 4.3 V vs Li<sup>+</sup>/Li at C-rates of 0.1, 0.2, 0.3, 0.5, 1, and 2 C (1 C = 200 mAh g<sup>-1</sup>) using Arbin LBT 21084a high-precision battery testing equipment. Cyclic voltammetry curves of all assembled cells were measured in the voltage range from 2.8 to 4.3 V vs Li<sup>+</sup>/Li at a scan rate of 0.1 mV s<sup>-1</sup>. The cycling stability of the created electrodes was analyzed by galvanostatic charging–discharging in the voltage range from 2.8 to 4.3 V at 0.2 C-rate charging and 1 C-rate discharging currents. At all galvanostatic charging–discharging tests created coin cells were charged at a constant current until 4.3 V vs Li<sup>+</sup>/Li and then at a constant voltage until the current decreased to 0.02 C-rate.

## Results and Discussion

**Calcination for NMC-sulphate particles.**—The thermal gravimetric analysis of the spray-dried NMC-sulphate particles performed in an air flow showed that complete dissociation of the produced material on metal oxide and sulphur dioxide occurs at about 825 °C after which the mass of the material decreased by about 61.2% (Fig. 1e). The mass losses before 200 °C (about 13.7%) and in the diapason of temperatures from 300 to 500 °C (about 9.5%) can be attributed to water evaporation and decomposition of organic impurities. Based on the thermal gravimetric analysis results, the temperature 825 °C was selected as the treatment temperature for the calcination of the produced spray-dried NMC-sulphate particles. The morphology of spray-dried NMC-sulphate particles is shown in Fig. 1. The applied spray-drying technology produces spherical NMC-sulphate particles with an average diameter of about 2.7 μm (Figs. 1a and 1d). After the calcination, the morphology of the spray-dried NMC-sulphate particles was changed. The smooth, spherical particles, previously observed for the spray-dried NMC-sulphate particles were converted to the highly agglomerated network of smaller particles due to the shrinking of the material at elevated temperatures (Figs. 1b and 1c). This led to a significant decrease in the average diameter of particles from 2.7 μm to 0.29 μm (Fig. 1g).

The EDS analysis was performed to confirm sulphur removal during the calcination at 825 °C and to investigate the composition of the produced NMC-oxide particles. EDS mapping patterns for the calcinated sample and EDS spectra of samples before and after calcination are shown in Fig. 2.

The analysis of obtained patterns and spectrums confirms the complete removal of sulphur during the calcination and a correct mixture of metals in required atomic ratios. However, the amount of oxygen in the calcinated material was significantly smaller than can be expected in the un-lithiated layered NMC oxide, where the atomic ratio between transition metals and oxygen (TM/O) is equal to 0.5. To investigate the mechanisms leading to oxygen deficiency during the calcination process, the isopropanol absorption bottle method was used in this study to determine the SO<sub>2</sub> and SO<sub>3</sub> concentrations in exhaust gases. The result of the analysis showed that sulphur is partly removed from the analysed material during the calcination process in the form of SO<sub>3</sub> gas. However, only 2.43 wt% of sulphur was removed in the form of SO<sub>3</sub> gas. The rest of the sulphur was removed in the form of SO<sub>2</sub> gas and collected in impingers filled with 100 ml of 3 vol% H<sub>2</sub>O<sub>2</sub> solution. The small detection of SO<sub>4</sub><sup>2-</sup> ions in the first impinger filled with 100 ml of 80 vol% isopropanol solution indicates small oxidation of the SO<sub>2</sub> to SO<sub>3</sub>, probably because of oxygen release during calcination of the spray-dried NMC-sulphate powder.

The XRD analysis of the calcinated sample showed that obtained materials mostly consist of three components, which are Mn<sub>0.025</sub>Co<sub>0.025</sub>Ni<sub>0.95</sub>O (04-023-7785, Cubic *Fm* $\bar{3}$ *m*), NiO (04-013-0886, hexagonal *R* $\bar{3}$ *m*) and MnCo<sub>2</sub>O<sub>4</sub> (04-028-9018, Cubic *Fd* $\bar{3}$ *m*) (Fig. 3). This composition almost corresponds to the composition of the material obtained after spray-pyrolysis of the metal chloride solution presented in Refs. 10, 12. However, we did not observe any other impurities caused by a reaction of the metal with SO<sub>2</sub> gas, even after a 12 h calcination process, as reported in Refs. 12 and 10 for NMC-oxide production from a metal chloride solution. The XRD spectrum peak matching showed that the amount of Mn<sub>0.025</sub>Co<sub>0.025</sub>Ni<sub>0.95</sub>O is 56% and MnCo<sub>2</sub>O<sub>4</sub> is 25%, and NiO is 19%, which is approximately equivalent to the molecular formula Ni<sub>0.72</sub>Co<sub>0.14</sub>Mn<sub>0.08</sub>O<sub>1</sub> and gives 0.937 TM/O ratio. This value is close to the measured TM/O ratio by EDS analysis, which is equal to 0.82.

Therefore, after investigation of the powder obtained after the calcination of spray-dried NMC-sulphate particles and analysis of

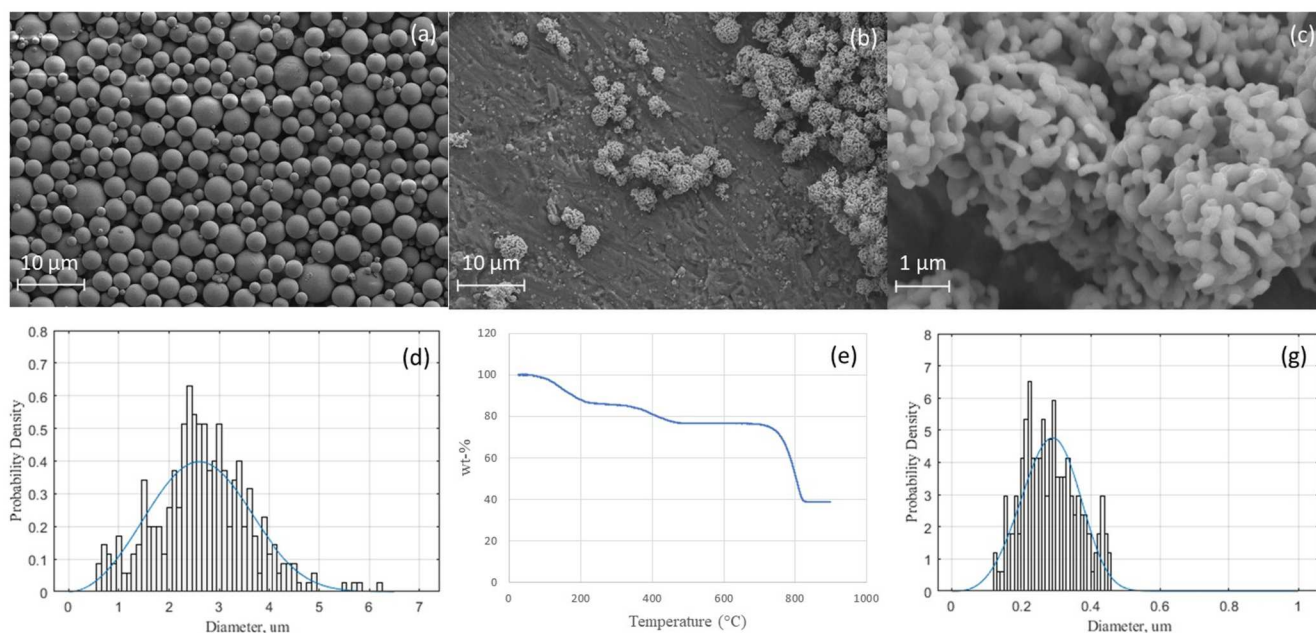


**Figure 1.** Morphology of obtained particles: spray-dried NMC-sulphate particles (a), NMC-oxide particles (b), (c); spray-dried NMC-sulphate particles size distribution (d) and result of the TG analysis for these particles in air (e) and NMC-oxide particles size distribution (g).

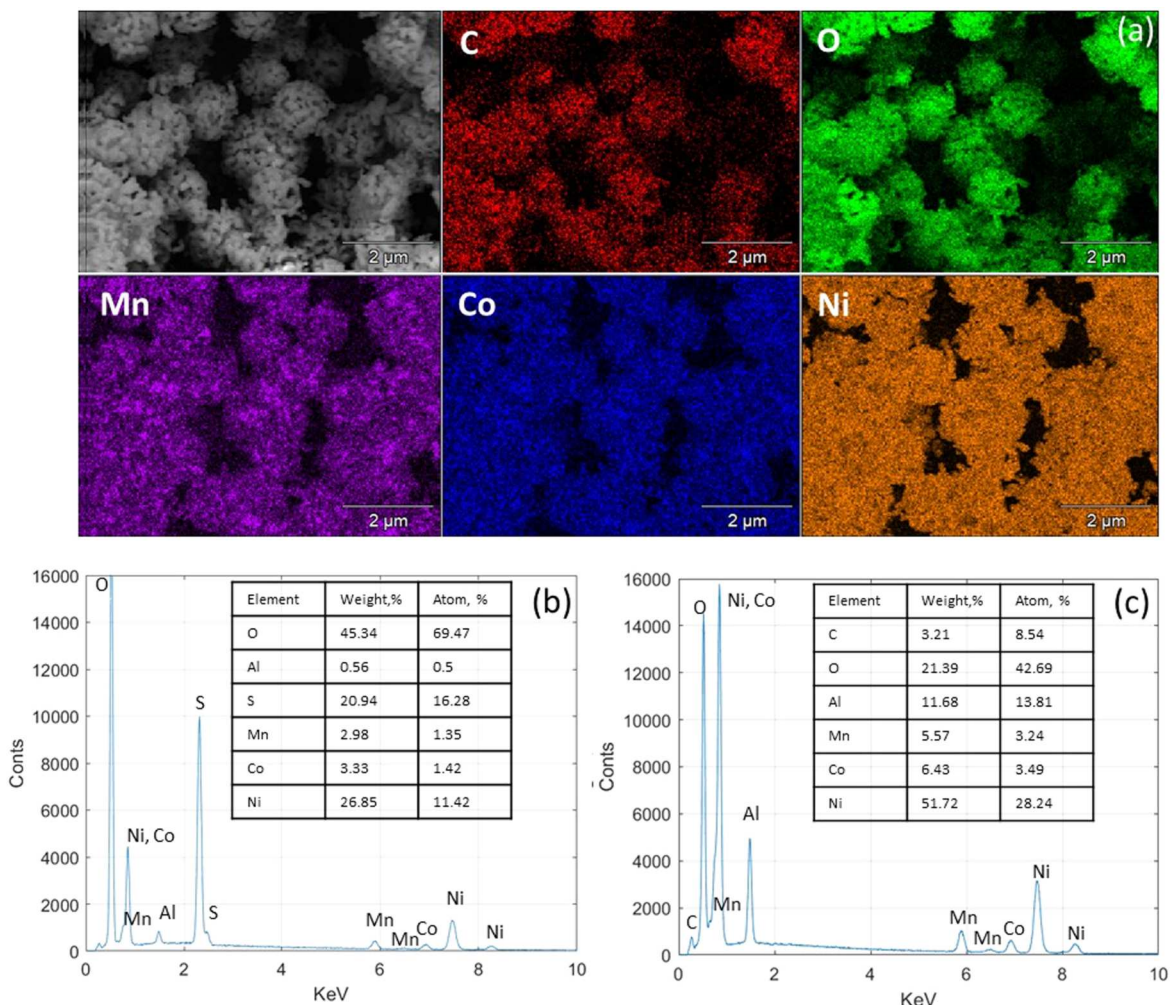


**Figure 2.** EDS mapping patterns of the NMC-oxide powder obtained after calcination (a), and EDS spectra of spray-dried NMC-sulphate powder before calcination (b) and NMC-oxide powder obtained after calcination (c).

the exhaust gasses, we can conclude that decomposition of NMC-sulphate particles at 825 °C leads to the formation of the mixture of metal oxides ( $\text{Mn}_{0.025}\text{Co}_{0.025}\text{Ni}_{0.95}\text{O}$ ,  $\text{MnCo}_2\text{O}_4$  and  $\text{NiO}$  or similar), release of  $\text{O}_2$  and  $\text{SO}_2$  gasses and a small amount of  $\text{SO}_3$  gas, which most probably was obtained after  $\text{SO}_2$  oxidation by  $\text{O}_2$ .

**Effect of lithium salt addition to the spray-dried NMC-sulphate powder before thermal treatment.**—The obtained during calcination process structures of the NMC-oxides (space group  $Fm\bar{3}m$ ) can be converted to the single crystal  $\text{LiNi}_{0.8}\text{Mn}_{0.1}\text{Co}_{0.1}\text{O}_2$  (SC-NMC) with layered  $\text{-NaFeO}_2$  structure (space group  $R\bar{3}m$ ) during the lithiation process as it was previously shown in research presented in 10, 12. However, the lithiation of small NMC oxide particles will lead to the production of the SC-NMC with a relatively high specific surface area. The high specific surface area can lead to serious side reactions, high electrolyte consumption and form an unstable cathode–electrolyte interface layer (CEI), which will harm cycling stability.<sup>18,19</sup> Therefore, to investigate the effect of the NMC oxide particle size on properties of the SC-NMC, produced after lithiation, the NMC oxide was mixed with a small amount of LiOH before calcination. The morphology of the particles, obtained after calcination, is shown in Fig. 4. The addition of LiOH before calcination changes the morphology and size of the particle, as can be seen in Fig. 4. This change can be caused by slight powder compressing because of the formation of  $\text{Li}_2\text{SO}_4$  during the reaction of the sulfur dioxide with lithium oxide and oxygen on the surface of NMC-oxide particles. The formation of the  $\text{Li}_2\text{SO}_4$  after calcination on the

surface of NMC-oxide was confirmed by EDS analysis (Fig. S1). After calcination, the  $\text{Li}_2\text{SO}_4$  can be completely washed by water to obtain the NMC-oxide particles. The samples obtained after washing are denoted as NMC-oxide-x, where x is the Li/TM ratio and it is equal to 0, 0.1, 0.2, 0.3, 0.5 and 0.9.

Analysis of the particle size distribution showed that even at Li/TM ratio equal to 0.1 significant bigger particles were obtained than without addition of the LiOH. The particle size distribution was calculated from SEM images by using ImageJ software and shown in Fig. S2. Despite of the fact that small addition of LiOH can lead to increase in the particle size, the relatively high amount of LiOH added before calcination leads to the formation of two types of particles. The particle size of the first type was decreased with an increase of Li/TM ratio, and the particle size of the second type was increased. Moreover, the EDS analysis showed that the increase in the Li/TM ratio leads to the non-uniform distribution of the Mn and Co in the NMC oxide (Fig. S3). Therefore, the addition of the LiOH with a Li/TM ratio more than 0.2 to the spray-dried NMC-sulphate particles before the calcination is not recommended for increasing the size of NMC-oxide particles.

**Conversion of materials from rock salt to layered structure.**—The in situ XRD analysis was performed to investigate the required condition of the lithiation process to guarantee the successful conversion of the NMC-oxides with space group  $Fm\bar{3}m$  to the required lithiated hexagonal  $\text{-NaFeO}_2$  structure with space group  $R\bar{3}m$ . The results of the study for the sample obtained after the

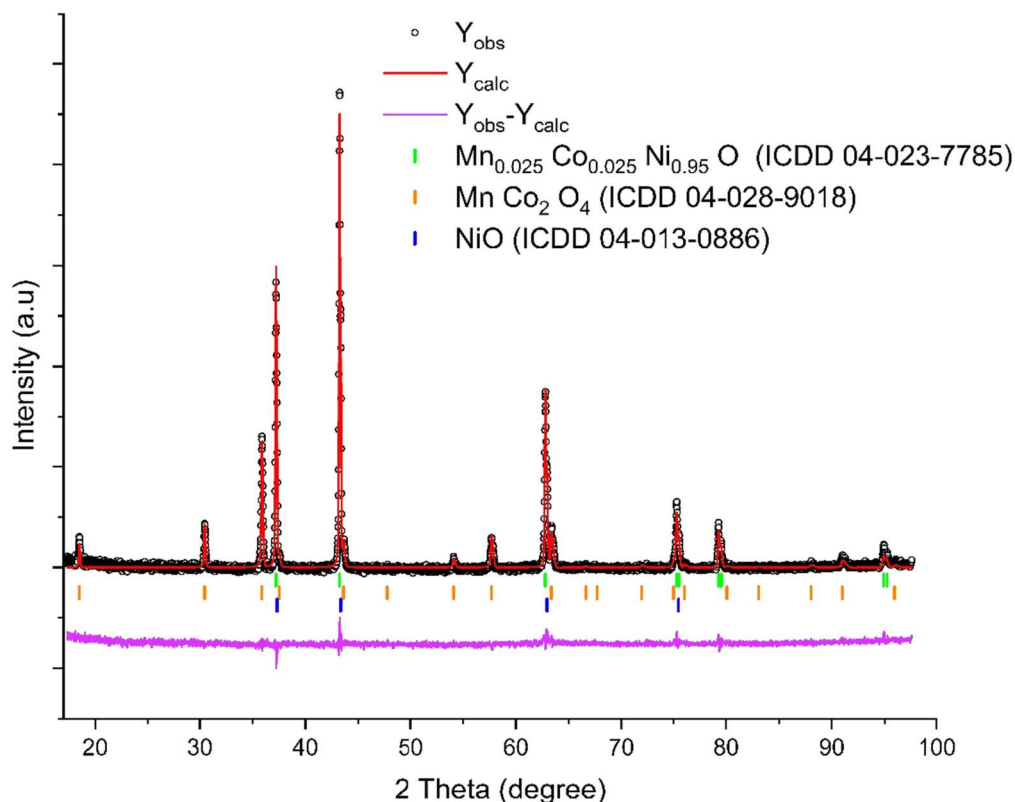


**Figure 3.** XRD spectrum of the NMC-oxide sample obtained after calcination of spray-dried NMC-sulphate sample.

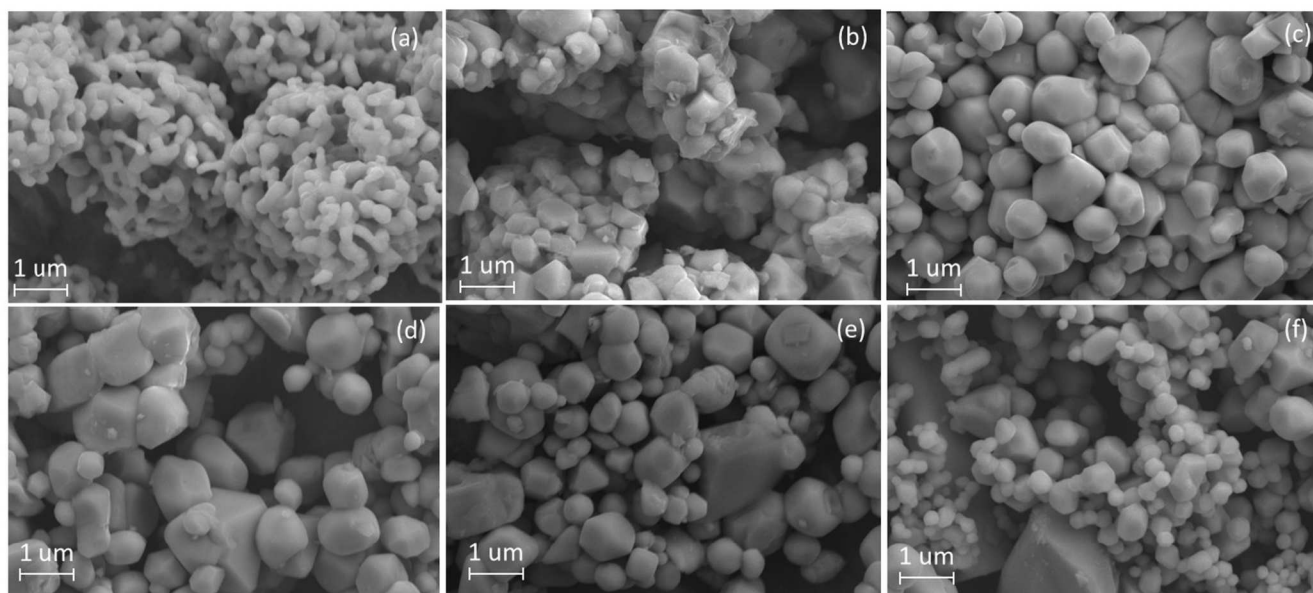


**Figure 4.** NMC oxide particle morphology with different amounts of LiOH added before calcination: NMC-oxide-0 (a), NMC-oxide-0.1 (b), NMC-oxide-0.2 (c), NMC-oxide-0.3 (d), NMC-oxide-0.5 (e) and NMC-oxide-0.9 (f).

calcination of the spray-dried NMC sulphate particles with LiOH (Li/TM = 0.5) are presented in Figs. 5 and 6.

As shown in Figs. 5 and 6, the decomposition of the LiOH appears at 300 °C and the 003, 006, 102, 104, 018, and 110 peaks, which correspond to the formation of the hexagonal  $\text{-NaFeO}_2$  structure (space group  $R\bar{3}m$ ), start to be observed at about 600 °C. The appearance of these peaks indicates the start of the precursor lithiation process. Moreover, the clear splitting of the 018 and 110 peaks after 750 °C indicates a well-organized layered structure.

However, the peaks, which correspond to the rock salt structure ( $Fm\bar{3}m$ ), disappear only after 850 °C, which can be used as an indicator of the minimum required temperature for the successful lithiation process. It should be noted that 850 °C is usually considered as a relatively high temperature for the NMC811 lithiation as the Ni/Li disordering is increased at such temperature, and Ni/Li disordering leads to the formation of the rock salt structure again.<sup>20</sup> Therefore, the lithiation time should be well optimized at such a temperature to decrease the Ni/Li disordering. After 250 °C

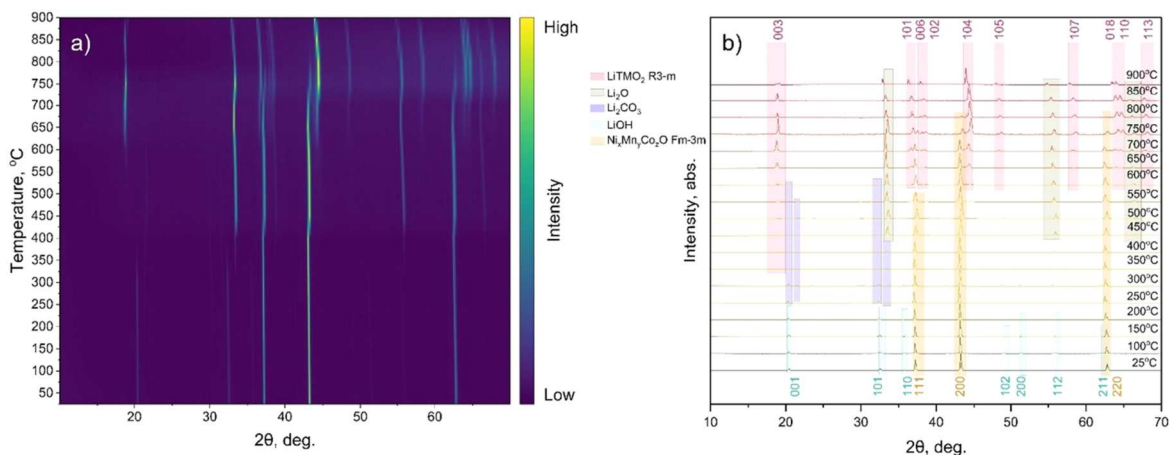


Figure 5. The counter-plot (a) and the XRD patterns (b) for the range of temperatures from 25 to 900 °C.

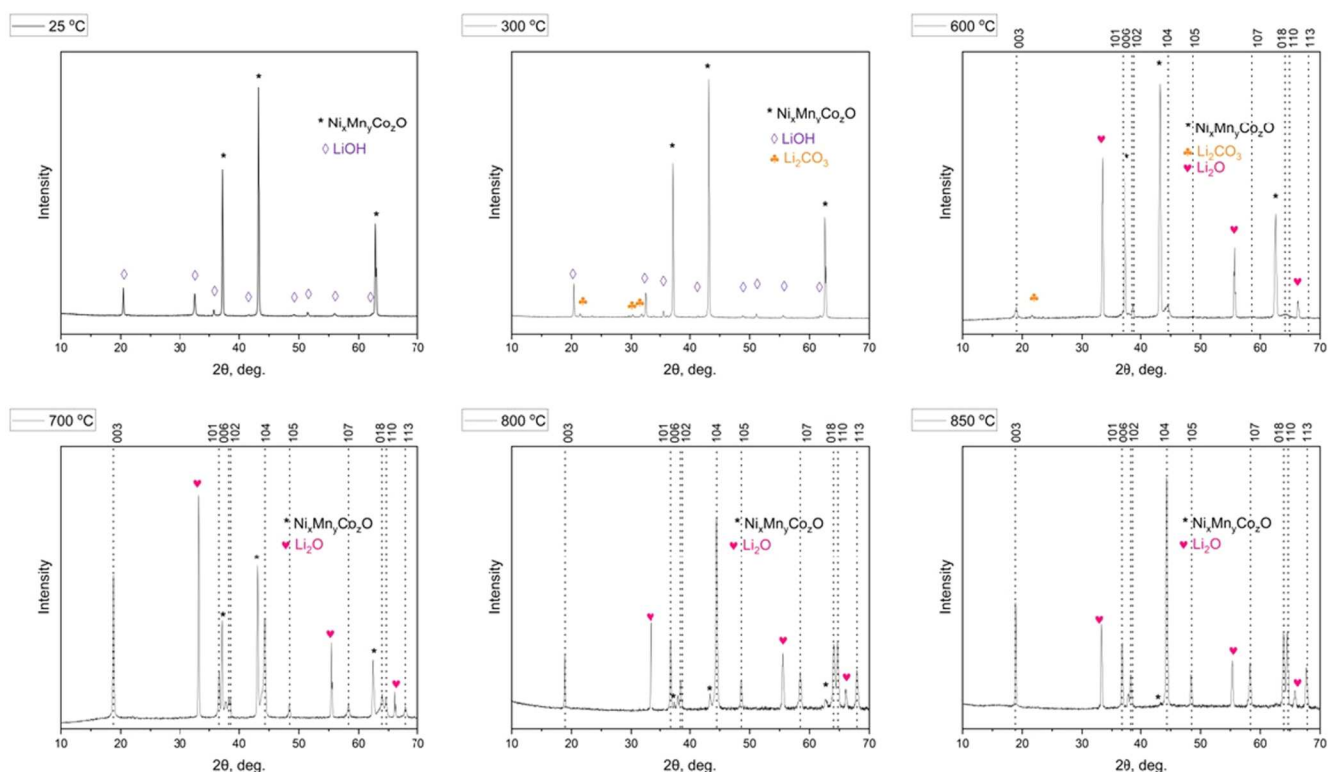


Figure 6. The XRD patterns at 25 °C (a), 300 °C (b), 600 °C (c), 700 °C (d), 800 °C (e), and 850 °C (f).

the lithium hydroxide transforms to Li<sub>2</sub>CO<sub>3</sub> because of the presence of atmospheric CO<sub>2</sub> in the in situ HT-XRD chamber. The additional phases observed on the XRD spectra after about 400 °C are attributed primarily to Li<sub>2</sub>O. This phase likely forms as an intermediate during the reaction between LiOH and the oxide precursor. With increasing temperature, the intensity of the Li<sub>2</sub>O peaks decreases significantly, suggesting that it is consumed as the layered NMC structure (R3m) forms more completely. However, these additional phases were not observed on the XRD spectrum of the sample after cooling anymore (Fig. S4), which suggests that Li<sub>2</sub>O transforms to Li<sub>2</sub>CO<sub>3</sub> and/or participates in the reaction of lithiation.

**Morphology and structural characterization of lithiated NMC-oxide powder.**—Based on the in situ XRD analysis, the lithiation of the NMC-oxides was done by a similar approach presented by Lui et al.<sup>15</sup> The two-step lithiation method was selected to decrease the release of oxygen and Li/Ni disordering that can be caused by

relatively high lithiation temperatures. The obtained samples after lithiation of the NMC-oxides samples were denoted as SC-NMC-x, where x indicates the amount of LiOH (in the form of Li/TM ratio) added to the spray-dried NMC-sulphate particles before calcination and is equal to 0, 0.1, 0.2, 0.3, 0.5 and 0.9. The SEM images of the lithiated samples were investigated to compare the morphology of synthesized samples (Fig. 7).

The negative effect of the LiOH addition to the NMC-sulphate particles before calcination on particle size uniformity was also observed in obtained samples after lithiation. The analysis of the particle size distribution (Fig. S5) showed that the LiOH addition before the calcination step increases the particle size of the lithiated material. Moreover, the specific surface area (SSA) and total pore volume of the samples with LiOH addition were significantly decreased compared to the SC-NMC-0 sample, as can be seen in Table I. The decrease in the SSA and total pore volume was achieved because of the decrease in the micro and mesoporosity of the powder

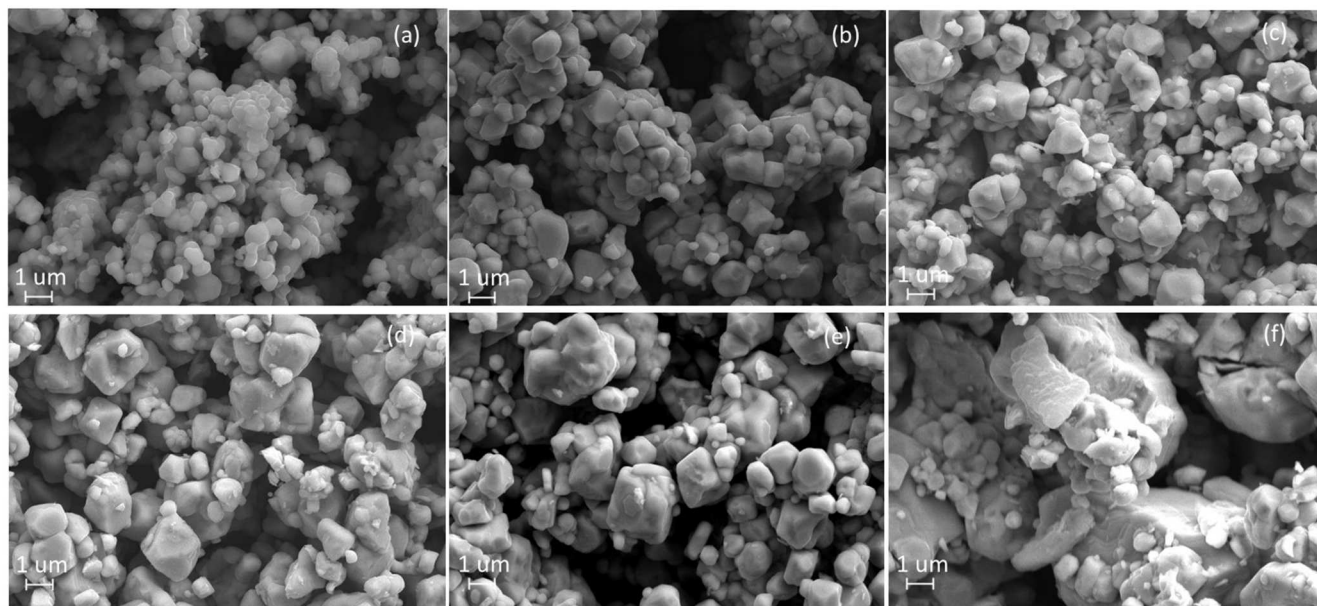


**Figure 7.** Lithiated NMC-oxide particles morphology: SC-NMC-0 (a); SC-NMC-0.1(b); SC-NMC-0.2 (c); SC-NMC-0.3 (d); SC-NMC-0.5 (e) and SC-NMC-0.9 (f).

produced by the calcination of the LiOH and NMC-sulfate particles mixture. Despite the achieved improvements in the particle size and SSA for the SC-NMC samples, it was not possible to achieve the similar SSA as it was obtained for the synthesis polycrystalline NCM811 powder (PC-NMC sample) using the co-precipitation method.

The decrease in the Mn and Co amounts during the addition of the LiOH to spray-dried spherical NMC-sulfate particles before calcination was also confirmed by ICP-OES. The results of the ICP-OES analysis are presented in Table II.

When the results of ICP-OES analysis of SC-NMC samples were compared with results for the PC-NMC sample the significantly lower amounts of sulfur and sodium in SC-NMC samples were observed than in the PC-NMC sample produced using the co-precipitation method. The increase of sulfur with an increase in the LiOH addition before calcination can be explained by less efficient washing of the  $\text{Li}_2\text{SO}_4$  from the material when the concentration of the  $\text{Li}_2\text{SO}_4$  increased with increasing amount of LiOH. The increase in aluminum concentrations in the samples can be explained by the reaction of LiOH with alumina crucible during the calcination of the LiOH and NMC-sulfate particles mixture.

An analysis of the XRD patterns of the produced samples, presented in Fig. 8, showed that all samples have diffraction peaks corresponding to the hexagonal  $\text{LiNi}_{0.8}\text{Co}_{0.1}\text{Mn}_{0.1}\text{O}_2$  structure with  $R\bar{3}m$  space group (Fig. 7). The XRD patterns of all samples were matched very well with  $\text{Li}_{1.01}\text{Ni}_{0.79}\text{Co}_{0.1}\text{Mn}_{0.1}\text{O}_2$  (ICDD file 01-090-4405). Only for the sample with a very high addition of the LiOH to the spray-dried NMC-sulfate powder before calcination (SC-NMC-0.9), a small diffraction peak at  $43.2^\circ$  was observed, which indicates the cation disordering and formation of the rock salt structures. The cation disordering was investigated by performing the Rietveld refinement for all considered samples (Fig. S6). The small values of R-factors and  $\chi^2$  indicated reasonably good refinement results. The slightly high values of R-factors and  $\chi^2$  for the sample SC-NMC-0.9 are caused by the small peak of the rock salt formation at  $43.2^\circ$ . The analysis showed a significant increase in Li/Ni disorder for SC-NMC-0.9. The obtained result was also in good agreement with another considered semi-quantitative parameter such as integrated intensities of the 003 and 104 reflections ( $I_{003}/I_{104}$ ), which for SC-NMC-0.9 is below 1.2 as it can be seen in Table III. The comparison of other lattice parameters was done by analyzing the  $c/a$  ratios, which signifies the degree of trigonal distortion. Good cationic

ordering is achieved if the value of this ratio is greater than 4.899.<sup>21</sup>

The  $c/a$  ratio for the samples obtained with the addition of LiOH to the spray-dried NMC sulphatic particles is slightly higher than this value for other considered samples, which indicates improving the ordering of the layered NMC cathode material with the addition of LiOH before the calcination step. However, the addition of LiOH before the calcination of NMC-sulfate particles also has a significant effect on 108 and 110 reflections ( $I_{108}/I_{110}$ ). The  $I_{108}/I_{110}$  ratio increases (from 0.92 to 1.04) with increasing of the LiOH amount, indicating that (110) facets become less exposed. The less exposed (110) facets affect negatively on  $\text{Li}^+$  diffusion and other electrochemical performances of the NMC cathode, as was previously reported by other researchers in 22, 23. The observed changes in XRD patterns of lithiated samples can be caused by decreasing the Mn amount in the composition of the obtained powders after calcination, which was confirmed by ICP-OES analysis. As was previously reported in 24, the decreasing of the Mn amount in the NMC cathode decreases the surface structural stability and chemical stability of the material.

**Electrochemical performance.**—An analysis of the morphology and structural characteristics of lithiated samples revealed negligible differences in parameters for samples SC-NMC-0.1, -0.2, and -0.3. The synthesis of the SC-NMC-0.2 and SC-NMC-0.3 samples necessitates the utilization of a greater quantity of lithium salt compared to that required to produce the SC-NMC-0.1 sample. Consequently, the analysis was constrained to the electrochemical characteristics of the SC-NMC-0 and SC-NMC-0.1 samples, which were identified as the most promising samples. Additionally, the analysis of the physical properties of SC-NMC-0.9 revealed a comparatively elevated  $\text{Li}^+/\text{Ni}^{2+}$  cation mixing ratio. Consequently, this specimen was excluded from the analysis of the electrochemical properties of the synthesized cathode materials. The measured first cycle performance and capacity retention after 200 cycles for selected samples are presented in Table IV and Fig. 9.

The analysis of the electrochemical characteristics of the selected samples demonstrated that sample SC-NMC-0 exhibited the optimal characteristics among the samples analyzed. Further analysis revealed that the electrochemical characteristics of the SC-NMC-0 are analogous to the electrochemical performance of the  $\text{LiNi}_{0.8}\text{Co}_{0.1}\text{Mn}_{0.1}\text{O}_2$  cathodes, as reported in previous studies (see Table S1). The comparison of the electrochemical characteristics of

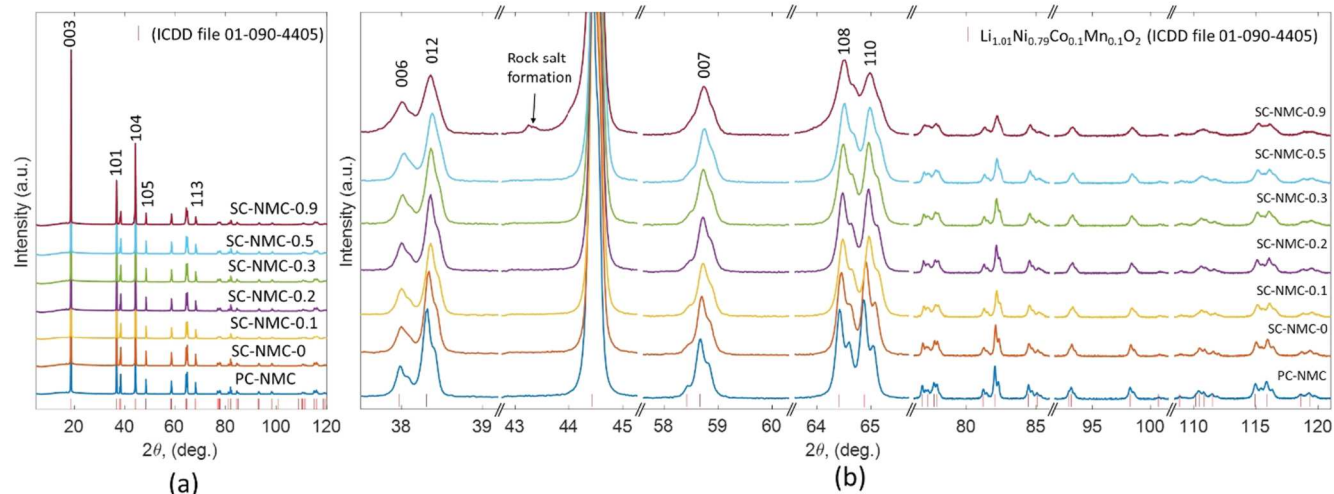


**Figure 8.** XRD patterns of the lithiated NMC-oxides (a) and magnified view showing the peak splitting and asymmetric peaks (b).

**Table I.** Particle size (D50), BET surface area and porosity of lithiated materials.

Samples	D (50), $\mu\text{m}$	SSA, $\text{m}^2\text{g}^{-1}$	Mean pore diameter, nm	Total pore volume, $\text{cm}^3\text{g}^{-1}$	Micropores (<2.2 nm), $\text{cm}^3\text{g}^{-1}$	Mesopores (2.2–50 nm), $\text{cm}^3\text{g}^{-1}$	Macropores (50 > nm), $\text{cm}^3\text{g}^{-1}$
SC-NMC-0	0.60	1.2	5.4	0.0014	0.0002	0.0010	0.0002
SC-NMC-0.1	0.94	0.6	5.6	0.0008	0.0001	0.0005	0.0002
SC-NMC-0.2	0.97	0.6	4.5	0.0006	0.0001	0.0004	0.0001
SC-NMC-0.3	1.08	0.6	5.8	0.0007	0.0001	0.0004	0.0002
SC-NMC-0.5	1.07	0.5	5.6	0.0008	0.0001	0.0005	0.0002
SC-NMC-0.9	0.97	0.4	6.1	0.0007	0.0000	0.0005	0.0002
PC-NMC	13.7	0.2	6.5	0.0007	0.0000	0.0004	0.0003

**Table II.** Metal contents of the lithiated NMC811 samples determined by ICP-OES.

Samples	Ni (mol%)	Co (mol%)	Mn (mol%)	Li/Me (mol ratio)	Na ( $\text{mg g}^{-1}$ )	S ( $\text{mg g}^{-1}$ )	Al ( $\text{mg g}^{-1}$ )
SC-NMC-0	80.56	9.57	9.87	0.941	0.28	0.422	0.029
SC-NMC-0.1	80.61	9.58	9.81	0.974	0.226	0.54	0.056
SC-NMC-0.2	80.58	9.59	9.83	0.966	0.223	0.55	0.053
SC-NMC-0.3	80.85	9.52	9.63	0.964	0.27	0.642	0.243
SC-NMC-0.5	80.79	9.52	9.69	0.961	0.221	0.806	0.183
SC-NMC-0.9	81.05	9.39	9.56	0.942	0.275	1.24	0.475
PC-NMC	80.63	9.65	9.72	0.928	0.746	1.21	0.011

samples SC-NMC-0 and SC-NMC-0.1 revealed that, despite having a larger particle size and smaller SSA, sample SC-NMC-0.1 exhibits initial electrochemical characteristics that do not significantly differ from those of SC-NMC-0. Both samples showed similar half-cell first cycle performances as PC-NMC sample. The SC-NMC-0.5 sample showed significantly worst half-cell first cycle performances, which most probably caused by decrease in the abundance of the exposed electroactive (110) facets in the SC-NMC-0.5 sample detected during XRD analysis. Electrochemical kinetics of the considered samples were studied using cyclic voltammetry (CV). The analysis of CV curves of considered samples showed clear H1, H2, and H3 phase transitions during lithium deintercalation and intercalation. The potential difference between the low voltage peak pair (H1→H2 and H2→H1) decreases in following samples order PC-NMC>SC-NMC-0.5>SC-NMC-0.1>SC-NMC-0. The reduction of the potential difference between the first pair of redox peaks implies faster kinetics according to the literature<sup>25</sup> and improves the rate-performance of the material as can be seen in Fig. 9c. The cycle life tests showed better cycling stability for the single crystal NMC

samples than for the polycrystalline NMC sample. After 200 cycles at 1 C rate current the specific discharge capacity retention of the SC-NMC-0 sample is 91%, unlike the specific capacity retention of the PC-NMC sample, which is 56.8%. The PC-NMC exhibits more severe capacity fading compared to SC-NMC, due to the crack formation in the polycrystalline structure. The obtained results correspond to the results presented in 26 where no significant changes in structure during cycling were observed for the single crystal NMC811, which confirms the superior resistance to mechanical degradation. In addition, the lower intensity of the redox peaks for the sample SC-NMC-0.5 observed in Fig. 9b indicates the decrease in charge transfer, which is also consistent with the results obtained by XRD analysis, which indicated less exposed (110) facets for SC-NMC-0.5 than for SC-NMC-0 and SC-NMC-0.1.

## Conclusions

Single crystal NMC811 cathode materials were successfully synthesized from metal sulfide precursors by spray drying and thermal treatment methods. The proposed approach has a significant

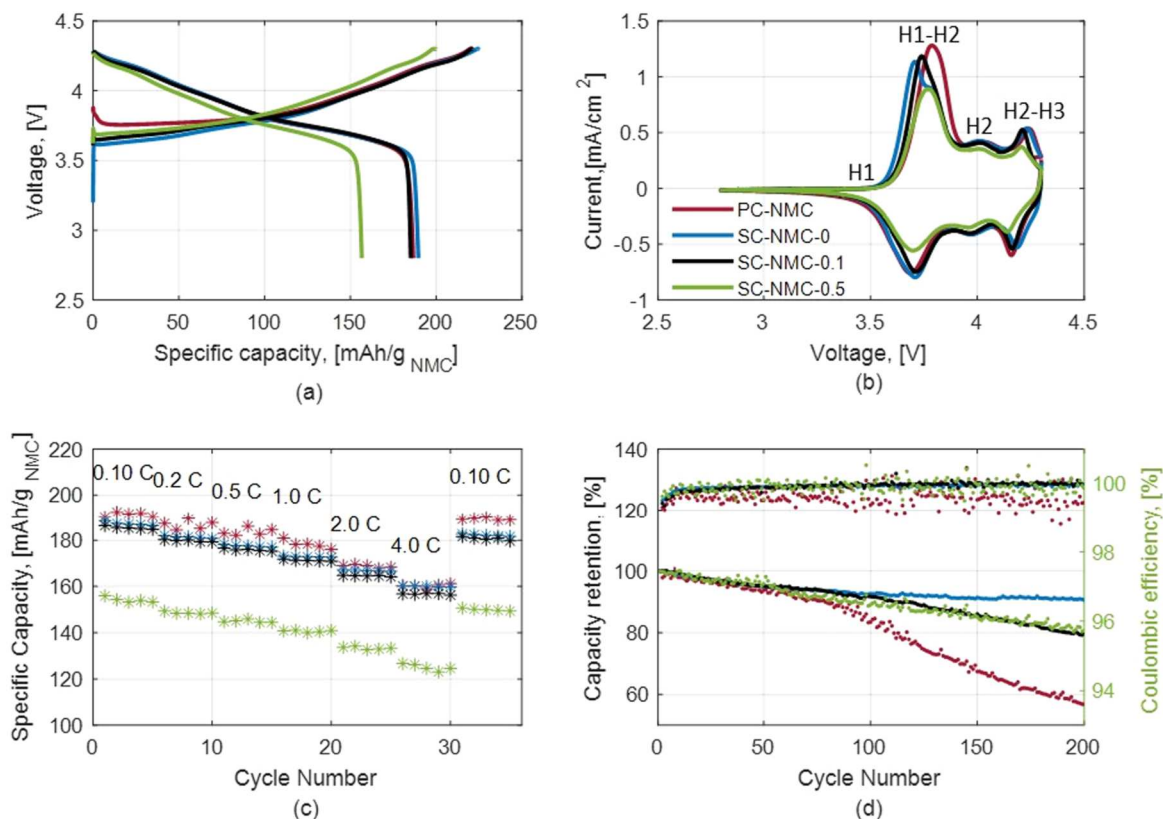


**Figure 9.** Electrochemical characteristics of the produced NMC samples. First charging-discharging cycle (a), CV curves (b) rate performances (c) and cycle life (d).

**Table III.** Tabulated fitting results of the XRD data of considered samples from Rietveld refinement.

Samples	$a, b$ (Å)	$c$ (Å)	Cell volume	$c/a$	$Li^+/Ni^{2+}$ cation mixing, %	$I_{003}/I_{104}$	$R_p, R_{wp}, R_{exp}, \chi^2$
SC-NMC-0	2.87117	14.20276	101.3963	4.94668	1.19	1.2924	7.69, 5.32, 2.45, 4.73
SC-NMC-0.1	2.86334	14.17086	100.6173	4.949066	1.23	1.2850	7.67, 5.21, 2.47, 4.47
SC-NMC-0.2	2.8693	14.1995	101.2408	4.948768	1.10	1.2875	7.85, 5.33, 2.47, 4.68
SC-NMC-0.3	2.86426	14.173	100.697	4.948224	1.18	1.2563	7.66, 5.29, 2.53, 4.38
SC-NMC-0.5	2.86916	14.19865	101.2246	4.948713	1.40	1.2616	7.77, 5.33, 2.53, 4.45
SC-NMC-0.9	2.86847	14.1959	101.1566	4.948945	2.15	1.1199	12.3, 8.75, 2.64, 11
PC-NMC	2.8726	14.204	101.5059	4.944649	0.70	1.2219	7.93, 5.45, 2.52, 4.68

**Table IV.** Half-cell first cycle performances and capacity retention % after 200 cycles.

Samples	CC 4.3 V / 0.1 C (mAh g <sup>-1</sup> )	DC 2.8 V / 0.1 C (mAh g <sup>-1</sup> )	ICE, %	DC after 200 cycles 2.8 V / 1 C (mAh g <sup>-1</sup> )	Average CE between 150 and 200 cycles, %
SC-NMC-0	224.5	189.6	84.45	149.9	99.973 ± 0.047
SC-NMC-0.1	220.8	185.2	83.88	131.3	99.998 ± 0.038
SC-NMC-0.5	199.7	156.7	78.47	114.9	99.916 ± 0.179
PC-NMC	221.0	186.7	84.48	100.1	99.235 ± 0.196

advantage over the widely used co-precipitation method as the conversion of the metal sulfates mixture to metal oxides mixture can be performed by removing the sulfur in form of the gas. In addition, the effect of the particle size on the electrochemical properties was analyzed. The particle size was increased by the addition of a small amount of LiOH during the calcination step, at which the metal sulfide mixture is converted to the metal oxide mixture. Despite the proposed method allowed to increase the particle size and decrease the SSA of the produced NMC811 cathode material, it also leads to

less exposed (110) facets. The negative effect of less exposed (110) facets of the produced material was more significant than the positive effect of the particle size increase, which leads to the deterioration in the chemical properties of the produced material. The best obtained result was corresponding to the material with smallest particles (about 0.60 μm), which has more exposed (110) facets. This material exhibited relatively good half-cell first cycle performances. The measured first cycle discharge specific capacity is equal to 189.6 mAh g<sup>-1</sup> and ICE is equal to 84.45%. Moreover, the produced

material has good rate performances with 159.8 mAh g<sup>-1</sup> specific capacity retention at 4 C-rate current and good cycle stability (90.6% of specific capacity retention after 200 cycles at 1 C-rate current).

### Acknowledgments

The authors acknowledge Business Finland BATCircle2.0 for the research funding 2021–2024 (University of Eastern Finland 44836/31/2020, University of Oulu 44612/31/2020, and Aalto university 44886/31/2020).

### ORCID

Kirill Murashko  <https://orcid.org/0000-0003-0177-8503>

### References

- M. H. Tahmasebi and M. N. Obrovac, "New insights into the all-dry synthesis of NMC622 cathodes using a single-phase rock salt oxide precursor." *ACS Omega*, **9**, 1916 (2024).
- J. Paulsen, E. Robert, D. Vanhoutte, D. NELIS, R. D. Palma, and D.-H. Kim, *Nitrate process for manufacturing transition metal hydroxide precursors*, WO2018167224A1 (2018), <https://patents.google.com/patent/WO2018167224A1/en#patentCitations>.
- S. N. Grigoriev et al., "Granulation of silicon nitride powders by spray drying: a review." *Materials*, **15**, 4999 (2022).
- H. Lee, P. R. Deshmukh, J. H. Kim, H. S. Hyun, Y. Sohn, and W. G. Shin, "Spray drying formation of metal oxide (TiO<sub>2</sub> or SnO<sub>2</sub>) nanoparticle coated boron particles in the form of microspheres and their physicochemical properties." *J. Alloys Compd.*, **810**, 151923 (2019).
- Z. LIU, G. HU, Z. PENG, X. DENG, and Y. LIU, "Synthesis and characterization of layered Li(Ni<sub>1/3</sub>Mn<sub>1/3</sub>Co<sub>1/3</sub>)O<sub>2</sub> cathode materials by spray-drying method." *Transactions of Nonferrous Metals Society of China*, **17**, 291 (2007).
- D. Li, Y. Sasaki, K. Kobayakawa, H. Noguchi, and Y. Sato, "Preparation, morphology and electrochemical characteristics of LiNi<sub>1/3</sub>Mn<sub>1/3</sub>Co<sub>1/3</sub>O<sub>2</sub> with LiF addition." *Electrochim. Acta*, **52**, 643 (2006).
- D. Li, Y. Kato, K. Kobayakawa, H. Noguchi, and Y. Sato, "Preparation and electrochemical characteristics of LiNi<sub>1/3</sub>Mn<sub>1/3</sub>Co<sub>1/3</sub>O<sub>2</sub> coated with metal oxides coating." *J. Power Sources*, **160**, 1342 (2006).
- J. Zhang, V. L. Muldoon, and S. Deng, "Accelerated synthesis of Li(Ni<sub>0.8</sub>Co<sub>0.1</sub>Mn<sub>0.1</sub>)O<sub>2</sub> cathode materials using flame-assisted spray pyrolysis and additives." *J. Power Sources*, **528**, 231244 (2022).
- Y. Liang et al., "Process engineering to increase the layered phase concentration in the immediate products of flame spray pyrolysis." *ACS Appl. Mater. Interfaces*, **13**, 26915 (2021).
- J. Zhu et al., "Flux-free synthesis of single-crystal LiNi<sub>0.8</sub>Co<sub>0.1</sub>Mn<sub>0.1</sub>O<sub>2</sub> boosts its electrochemical performance in lithium batteries." *J. Power Sources*, **464**, 228207 (2020).
- B. You et al., "A fresh one-step spray pyrolysis approach to prepare nickel-rich cathode material for lithium-ion batteries." *ACS Appl. Mater. Interfaces*, **11**, 14587 (2023).
- T. Li, X. Li, Z. Wang, and H. Guo, "A short process for the efficient utilization of transition-metal chlorides in lithium-ion batteries: a case of Ni<sub>0.8</sub>Co<sub>0.1</sub>Mn<sub>0.1</sub>O<sub>1.1</sub> and LiNi<sub>0.8</sub>Co<sub>0.1</sub>Mn<sub>0.1</sub>O<sub>2</sub>." *J. Power Sources*, **342**, 495 (2017).
- J. Zhao et al., "In situ probing and synthetic control of cationic ordering in Ni-rich layered oxide cathodes." *Adv. Energy Mater.*, **7**, 1601266 (2017).
- J. Leng et al., "Highly-dispersed submicrometer single-crystal nickel-rich layered cathode: spray synthesis and accelerated lithium-ion transport." *Small*, **17**, 2006869 (2021).
- A. Liu, N. Zhang, J. E. Stark, P. Arab, H. Li, and J. R. Dahn, "Synthesis of Co-free Ni-rich single crystal positive electrode materials for lithium ion batteries: part I. Two-step lithiation method for Al- or Mg-doped LiNiO<sub>2</sub>." *J. Electrochem. Soc.*, **168**, 040531 (2021).
- P. Laine et al., "Co-precipitation of Mg-doped Ni<sub>0.8</sub>Co<sub>0.1</sub>Mn<sub>0.1</sub>(OH)<sub>2</sub>: effect of magnesium doping and washing on the battery cell performance." *Dalton Trans.*, **52**, 1413 (2023).
- Environmental Protection Agency, (1996), USA <https://www.epa.gov/sites/default/files/2015-07/documents/epa-method8.pdf>.
- Z. Meng, X. Ma, L. Azhari, J. Hou, and Y. Wang, "Morphology controlled performance of ternary layered oxide cathodes." *Commun Mater*, **4**, 90 (2023).
- J. Wang, X. Lu, Y. Zhang, J. Zhou, J. Wang, and S. Xu, "Grain size regulation for balancing cycle performance and rate capability of LiNi<sub>0.9</sub>Co<sub>0.05</sub>Mn<sub>0.045</sub>O<sub>2</sub> single crystal nickel-rich cathode materials." *Journal of Energy Chemistry*, **65**, 681 (2022).
- Y.-S. Chen, R. Dominko, M. Marczewski, and W. Wiczonek, "Optimizing high-energy lithium-ion batteries: a review of single crystalline and polycrystalline nickel-rich layered cathode materials: performance, synthesis and modification." *Appl. Phys. A*, **130**, 740 (2024).
- C. Julien, A. Mauger, K. Zaghib, and H. Groult, "Optimization of layered cathode materials for lithium-ion batteries." *Materials*, **9**, 595 (2016).
- M. Jiang et al., "Synthesis of Ni-rich layered-oxide nanomaterials with enhanced Li-ion diffusion pathways as high-rate cathodes for Li-ion batteries." *ACS Appl. Energy Mater.*, **3**, 6583 (2020).
- F. Li et al., "Ni-rich layered oxide with preferred orientation (110) plane as a stable cathode material for high-energy lithium-ion batteries." *Nanomaterials*, **10** (2020).
- J. Zheng, W. H. Kan, and A. Manthiram, "Role of Mn content on the electrochemical properties of Nickel-Rich layered LiNi<sub>0.8-x</sub>Co<sub>0.1</sub>Mn<sub>0.1+x</sub>O<sub>2</sub> (0.0 ≤ x ≤ 0.08) cathodes for lithium-ion batteries." *ACS Appl. Mater. Interfaces*, **7**, 6926 (2015).
- D. Zhang et al., "Effect of Ti ion doping on electrochemical performance of Ni-rich LiNi<sub>0.8</sub>Co<sub>0.1</sub>Mn<sub>0.1</sub>O<sub>2</sub> cathode material." *Electrochim. Acta*, **328**, 135086 (2019).
- X. Shi et al., "Phase-transition-induced crack formation in LiNi<sub>0.8</sub>Mn<sub>0.1</sub>Co<sub>0.1</sub>O<sub>2</sub> cathode materials: a comparative study of single-crystalline and polycrystalline morphologies using *Operando* X-ray CT." *ACS Appl. Energy Mater.*, **7**, 11144 (2024).